

## Biogeochemical patchiness at the sea surface

A. Mahadevan

Department of Applied Mathematics and Theoretical Physics, University of Cambridge, Cambridge, UK

Ocean Process Analysis Laboratory, University of New Hampshire, Durham, New Hampshire, USA

J. W. Campbell

Ocean Process Analysis Laboratory, University of New Hampshire, Durham, New Hampshire, USA

Received 21 September 2001; accepted 11 December 2001; published 10 October 2002.

[1] The surface distributions of many tracers in the ocean are highly correlated in time and space on meso ( $\sim 100$  km) and smaller scales (Figure 1). However, their characteristic scales of variability differ. Some variables like sea surface chlorophyll (Chl) are very fine-scaled or patchy, while others like sea surface temperature (SST) are not. We characterize the patchiness of a distribution quantitatively by the dependence of the variance  $V$  on the length scale  $L$  as  $V \sim L^p$ ; smaller  $p$  corresponds to greater patchiness. Using scaling and a numerical model we show that patchiness,  $p$ , varies with the characteristic response time  $\tau$  of the tracer to processes that alter its concentration in the upper ocean as  $p \sim \log \tau$ . This suggests that sea surface Chl is more patchy (has smaller  $p$ ) than SST at mesoscales because the characteristic time scale of phytoplankton growth in response to the availability of nutrients is less than that for the equilibration of temperature in response to heat fluxes. Similarly, sea surface dissolved oxygen ( $O_2$ ) exhibits more fine-scaled variability than total dissolved inorganic carbon ( $TCO_2$ ) because  $O_2$  equilibrates with the atmosphere much more rapidly than  $TCO_2$ . Tracers that are more patchy require higher resolution to model and sample; the sampling or model grid spacing required scales as  $\exp(-1/\log \tau)$ . The quantitative relationship between  $p$  and  $\tau$  can be used to relate various biogeochemical distributions, particularly to those that are remotely sensed, and to deduce biogeochemical response times of various tracers or plankton species from the characteristics of their distributions in space or time.

**INDEX TERMS:** 4808 Oceanography: Biological and Chemical: Chemical tracers; 4520 Oceanography: Physical: Eddies and mesoscale processes. **Citation:** Mahadevan, A., and J. W. Campbell, Biogeochemical patchiness at the sea surface, *Geophys. Res. Lett.*, 29(19), 1926, doi:10.1029/2001GL014116, 2002.

### 1. Introduction

[2] Many ocean properties like temperature, salinity, nitrate, phosphate,  $TCO_2$ ,  $O_2$ , dissolved organic carbon and nitrogen (DOC and DON) have the common trait that their concentrations change rapidly with depth just below the mixed layer. This is because these substances are typically forced or modified in the upper ocean or at the air-sea interface, and vertical mixing that communicates these changes with the interior, occurs at very small rates. Over long times, the mean vertical concentration profiles of these substances are set by the balance between their rate of

production or removal in the upper ocean and the rate of exchange between the upper ocean and the interior. But their concentration at the sea surface is altered, often episodically, on shorter time scales (of days to weeks) by (i) the upwelling of waters with substantially different properties, and (ii) processes like biological production and air-sea exchange that modify the tracers.

[3] Upwelling associated with fronts and dynamical instabilities is instrumental in transporting nutrients to the surface in the pelagic ocean [Lévy *et al.*, 2001; Mahadevan and Archer, 2000]. It occurs on sub-mesoscales, i.e., scales of order 1–10 km, and introduces anomalies and variance at small scales in the biogeochemical concentrations at the sea surface. Processes like air-sea exchange and biological production alter the biogeochemical properties in the upper ocean and tend to erode the anomalies introduced by upwelling. Physical variables like temperature and salinity are altered by heat and evaporation/precipitation (E-P) fluxes at the surface. Nitrate, phosphate,  $O_2$ ,  $TCO_2$ , alkalinity and Chl, are modified by biological production of phytoplankton in the upper ocean. In oligotrophic regions, high values of Chl are seen where upwelling brings nutrients and cold water to the surface. Dissolved gases like  $O_2$  and  $CO_2$  are subject to air-sea exchange at the surface, albeit they equilibrate at different rates.

[4] The small-scale variance in the surface concentration field of tracers that is introduced by upwelling, is of scales finer than those associated with horizontal advection. Here, upwelling, and the response it solicits, is responsible for the introduction of sharp gradients and variance in the sea surface concentrations of various tracers within a limited region of the pelagic ocean. Horizontal advection tends to spread and stir the concentration anomalies. This differs from the case where variance is introduced at scales larger than those associated with horizontal advection (due to geographical variation, for example) and is stirred into finer scale filamentous structures by horizontal advection [Abraham, 1998].

[5] There is a strong correlation between the various sea surface properties (Figure 1) that results from the common dynamics and their qualitatively similar concentration gradients in the vertical. But they also differ, most significantly in the fact that they exhibit different degrees of patchiness, or variability at a given length scale. Several studies [Denman *et al.*, 1977; Folt and Burns, 1999; Young *et al.*, 2001] attribute the patchiness of biological variables like phytoplankton (in comparison to physical variables like temperature) to the fact that their distributions are affected not only by the flow, but also by reproduction. Here we show that

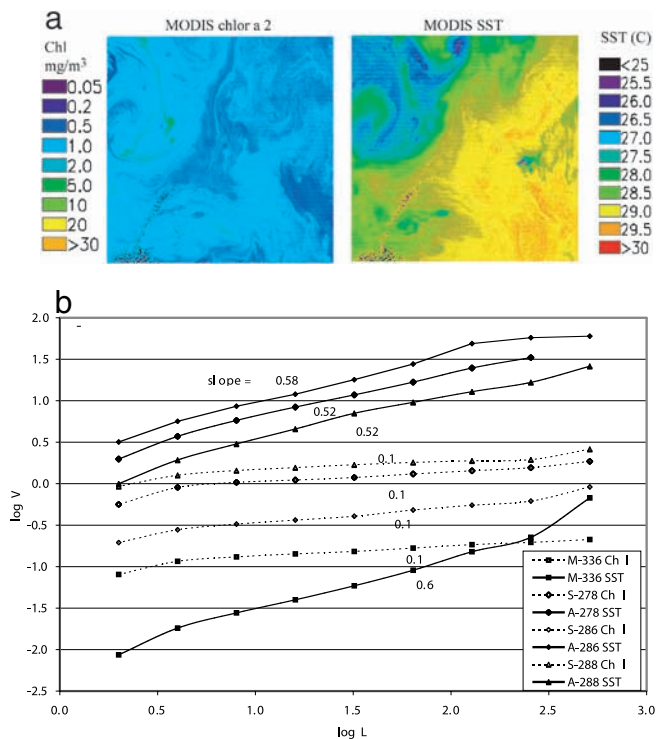


**Figure 1.** Top: Simultaneous satellite images of sea surface temperature (SST) and chlorophyll (Chl) in the Arabian Sea acquired by the Moderate Resolution Imaging Spectroradiometer (MODIS) on December 1, 2000. The color scale is logarithmic for Chl, but linear for SST. The size of the domain is  $512 \times 512 \text{ km}^2$  within which the variance-scale relationship was analyzed (lower plot). The M-336 curves are based on the MODIS data shown above. (Chl: dotted, SST: bold.) In addition, we show results for three concurrent AVHRR (A-278, A-286, and A-288) SST and Sea WiFS (S-278, S-286, and S-288) Chl images from the N. Atlantic in October 2000. The length scales analyzed range from 2 to 512 km. The slopes indicated are estimated for lines fitted to the points between  $L = 4 \text{ km}$  and  $256 \text{ km}$ .

spatial heterogeneity among various tracers can result from differences in the characteristic response times of the tracers to processes altering them. Even substances acted on by the same processes differ in their distributions when their rates of response differ. The wide range of process-response times that exist among various tracers in the ocean, is thus one of the main reasons for differences in the patchiness of biogeochemical tracer distributions.

## 2. Quantifying Variability

[6] We introduce a simple approach to characterize and compare the spatial heterogeneity among tracers, which in contrast to methods like spectral analysis [Platt and Denman, 1975; Gower et al., 1980], semi-variogram analysis [Yoder et al., 1987; Yoder et al., 1993; Glover et al., 2002; Deschamps et al., 1981] and autocorrelation analysis [Campbell and Esaias, 1985], does not invoke the assumption of isotropy in the distributions. This method characterizes the spatial variance  $V$  in terms of the characteristic length scale,  $L$ . We first calculate the variance over an area

of dimension  $L$ , and then over subdomains of size  $L/2$ ,  $L/4$ ,  $L/8$ , ..., into which the region is partitioned.  $V(L)$  is then the average variance contained within all subdomains of area  $L^2$  that comprise the domain, and is normalized by the total variance in the domain. We analyze the variance-scale relationships in several satellite images of sea surface Chl and SST (Figure 1). For length scales between 4 and 256 km,  $V$  varies more or less linearly with  $L$  in log-log space, suggesting a power law relationship of the form

$$V \sim L^p, \quad (1)$$

where  $p > 0$ . Variations in the exponent reflect differences in the percentage of total variance retained at small scales. A distribution whose variance  $V(L)$  falls on a line with small slope,  $p$ , in the log-log space, is more fine-scaled or patchy than one that has a steeper slope. In the satellite images analyzed, Chl and SST are highly correlated because Chl is produced in response to upwelling of nutrient-rich subsurface waters that are cold relative to the surface. But the slopes of the log-log  $V(L)$  curves for SST are greater than those for Chl from the same scene, indicating that Chl is more patchy than SST over the range of scales analyzed. While the actual variance of a single variable may vary by as much as two orders of magnitude from one time or place to another, the exponents  $p$  (which are the slopes shown in Figure 1) tend to vary much less.

## 3. Modeling and Results

[7] Using a simple model, we now explain the differences in tracer patchiness. The evolving distribution of a tracer in a flow field is described by  $\partial c/\partial t + \mathbf{u} \cdot \nabla c = S$  where  $c$  is the tracer concentration,  $\mathbf{u}$  is the fluid velocity, and  $S$  represents a source (or sink) term. We neglect diffusion on the large scales under consideration. In many cases, this source term  $S$ , represents the uptake of the tracer or its restoration to some value, and depends on (i) the concentration of the quantity itself, which is in turn linked to the supply rate from the deeper ocean, and (ii) the characteristic time scale  $\tau$  or rate of the alteration process, be it biological production, chemical equilibration, or air-sea flux. Using the example of a nutrient-like tracer (nitrate), we model its source as  $S = -\tau^{-1}c$  in the euphotic layer (taken to be the upper 95 m in our model), where  $\tau$  is a characteristic biological time scale of growth or nutrient uptake. We initialize the tracer to resemble nitrate in the oligotrophic ocean; it is absent from the upper 95 m and beneath this it increases rapidly with depth to attain a maximum at approximately 500 m. When the tracer is advected into the euphotic zone, it is depleted (due to biological uptake) at the rate  $\tau^{-1}c$ . The consumed tracer is redistributed at depth to account for remineralization.

[8] Let  $c'$  and  $c_\infty$  represent the anomalous (variation from the sea surface mean,  $\bar{c}$ ) value of the tracer concentration at the sea surface and at depth, respectively, normalized by  $\bar{c}$ . Then we can express a balance between vertical tracer advection and sources (in the tracer equation presented at the beginning of the section) as  $W/h(c' - c_\infty) \sim -c'/\tau$  where  $W$  is the characteristic vertical velocity,  $h$  is the characteristic vertical scale, and  $(c' - c_\infty)/h$  represents the vertical gradient. Rearranging terms and taking their logarithm gives  $\log c' \sim \log c_\infty + \log \bar{\tau}$ , where  $\bar{\tau} \equiv \tau W/h$  is the

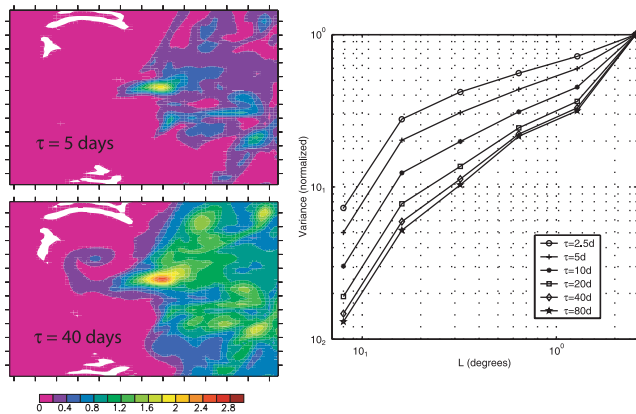


**Figure 2.** Left: Concurrent views of the model surface concentration (averaged over the upper 95 m) of two of the nutrient-like tracers with uptake times  $\tau = 5$  days and 40 days. The tracer with larger  $\bar{\tau}$  is less patchy and has higher surface concentration. Right: Log-log plot of the average variance  $V$  v.s.  $L$  for tracers with different  $\tau$  (two of which are shown on the left). Each tracer is characterized by a different slope  $p$ .

ratio of the tracer (biogeochemical) time scale to the vertical advection time scale, the inverse of which is known sometimes as the Damköhler number. For simplicity, we assumed here that is significantly less than 1. The variance  $V \sim c^2$  and the patchiness  $p \equiv \log V / \log L$ . Therefore

$$p \sim \log c_{\infty} + \log \bar{\tau}, \quad (2)$$

if  $p$  is assumed to be more or less constant over the range of scales considered. The contribution of horizontal advection to increasing the variance at the sea surface is neglected. It could be significant when  $\tau$  exceeds the time scale associated with the formation of fine-scaled stirring filaments, but tracers with relatively large  $\tau$  are not considered here, in consistency with our previous simplification that considers  $\bar{\tau} < 1$ . Since we compare different tracer distributions that are subject to the same flow field, we do not differentiate between  $\tau$  and  $\bar{\tau}$  in our presentation of the model results.

[9] To verify the scaling relation (2), we couple the above described model of a nutrient-like tracer  $c$ , to a three-dimensional non-hydrostatic ocean model [Mahadevan *et al.*, 1996]. It is configured to simulate a baroclinically unstable upper ocean front (at approximately 4 km resolution) in a periodic channel of dimension 285 km  $\times$  258 km. We examine the dependence of the tracer distribution on  $\tau$  by using six different values of  $\tau$  in the simulation:  $\tau = 2.5, 5, 10, 20, 40$  and 80 days. The tracers with different  $\tau$  are identically initialized and advected. When  $\tau$  is small, the upwelled tracer that has an anomalous concentration in relation to the surrounding surface water is modified rapidly and restored to the ambient sea surface condition. In the oligotrophic ocean, for example, upwelled nutrients are rapidly (on a time scale of 3–7 days) taken up by phytoplankton so as to restore oligotrophy. The anomalous tracer quantity in the surface ocean remains small, and appears only on the small scale at which upwelling occurs. As  $\tau$  is

increased, the anomalous tracer value and the size of the anomalous patches at the surface increase due to the expansion of the upwelling region and further supply from the subsurface, as well as horizontal advection.

[10] At various times in the simulation, we analyze the surface distributions of the tracer (two-dimensional fields of the average tracer concentration in the upper 95 m) using the variance method (Figure 2). Plots of the patchiness index  $p$  v.s.  $\log \tau$  at different instances of time (shown in the left panel of Figure 3) are consistent with (2); smaller  $\tau$  results in greater patchiness and  $p \sim \log \tau$ . But the curves differ because of their dependence on the flow field which is changing with time.

[11] Tracers that have more patchy distributions require higher resolution to model or sample. If  $\Delta$  is a non-dimensionalized horizontal length scale at which a fixed proportion (say 80%) of the variance of the region is captured, then substituting  $V = 0.8$  and  $\Delta$  into (1), we get  $\log \Delta \sim -1/p$ , which when combined with (2) gives

$$\Delta \sim \exp(-1/\log \bar{\tau}), \quad (3)$$

if we assume  $c_{\infty}$  to be more or less constant amongst the tracers considered. Thus, if we take the characteristic time for biological growth in response to nutrient availability to be about 3 days, and the relaxation time scale for temperature to surface forcing to be about 30 days, we can estimate that the factor of 10 difference in the response

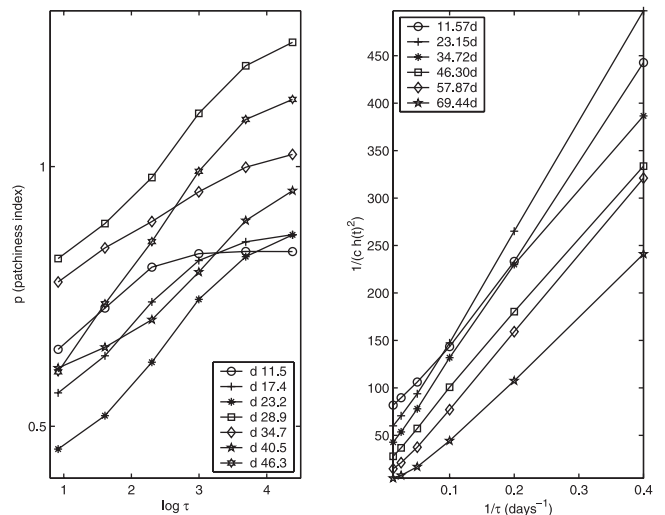


**Figure 3.** Left: The approximate slope  $p$ , of the  $V$ - $L$  curves (Figure 2), estimated for the central portion of each curve (neglecting the two end points), plotted against  $\log \tau$ . The different curves represent different times in the simulation, indicated by ‘days’ in the legend. The linear relationship between  $p$  and  $\log \tau$  is poor at initial times (less than  $\tau$ ) in the simulation and deteriorates at large  $\tau$ , as expected. Right: The relation between the mean sea surface concentration of a tracer,  $\bar{c}$ , and  $\tau$  is tested by plotting  $c_{\infty} D / \bar{c} h^2$  v.s.  $1/\tau$  at different times in the simulation.  $\bar{c}$  is taken to be the mean over the upper 95 m in the model.  $D$  and  $c_{\infty}$  are taken to be constant, while  $h$  is assumed to increase linearly with time to account for the decay in the flow field and adjustment of the nutrient profile with time.

times requires that the resolution for modeling or sampling new production be finer than that for temperature by a factor of approximately 4. Similarly for dissolved gases whose concentrations are changed by air-sea exchange at the sea surface, the typical equilibration times determine the model resolution needed. In the absence of biological effects, we could say that  $O_2$  which takes about a month to equilibrate over typical mixed layer depths, requires about 4 times more resolution than  $TCO_2$ , for which the equilibration time is about 10 months.

[12] Larger values of  $\tau$  result in slower nutrient uptake, and thus greater quantities of nutrient in the euphotic zone. Assuming a steady state average concentration of nutrient in the upper layer and averaging the tracer equation at the beginning of section 3 with  $S = -\tau^{-1}c$  over the entire surface layer, gives the balance

$$\frac{D}{h^2}(\bar{c} - c_\infty) \sim -\frac{\bar{c}}{\tau} \Rightarrow \bar{c}/c_\infty = 1/\left(1 + \frac{h^2}{D\tau}\right). \quad (4)$$

Here  $\bar{c}$  is the average upper ocean tracer concentration,  $D$  is an effective vertical diffusivity, and  $h$  a characteristic height, so that the first term denotes the integrated effect of vertical advection. In Figure 3 (right) we plot  $c_\infty D/\bar{c}h^2$  vs.  $1/\tau$  at different times in the model simulation. The findings are in agreement with (4).

#### 4. Discussion and Conclusions

[13] The results derived here are independent of the specific process modifying the tracer and can be generalized to any tracer whose upper ocean source or sink can be parameterized in terms of a characteristic e-folding time  $\tau$ . The uptake or production of biological tracers like nutrients,  $TCO_2$ ,  $O_2$ , alkalinity and Chl can be quantified in terms of a biological uptake or growth time scale. The change in the concentrations of  $O_2$  and  $TCO_2$  due to air-sea gas exchange can be parameterized in terms of a time scale that is the ratio of the mixed layer depth to piston velocity (times the Revelle factor to account for buffering in the case of  $TCO_2$ ), while the change in physical properties like temperature and salinity is often modeled by restoration with an e-folding time scale. Multiple time scales arising from several processes can be combined using their non-dimensionalized harmonic mean [Mahadevan and Campbell, 2002]. In the ocean, biological uptake time scales are typically much shorter than the response time of SST to heat fluxes. This explains why biological variables like sea surface Chl are more patchy than SST at mesoscales. Similarly sea surface  $O_2$  is expected to be more patchy than  $TCO_2$  because although both are affected by biological production,  $O_2$  equilibrates with the atmosphere about 10 times faster than  $TCO_2$ . Consequently,  $O_2$  and Chl require more sampling resolution than  $TCO_2$  and SST.

[14] The relationships derived here in terms of spatial distributions can be extended to the temporal context, using intermittency as the analog of patchiness, and then explored using time series data. The logarithmic dependence on response time implies that tracers with short response times are not only more patchy, but their distributions are also more sensitive to changes in their response time. In models, therefore, it is the faster responding tracers, like the bio-

logical variables, whose response times need to be represented more accurately. This makes biological modeling particularly challenging.

[15] The relationship between the response time of a tracer and its surface distribution can be used to relate different biogeochemical tracers in the ocean and to deduce the characteristics of certain distributions from other satellite-derived variables. Differences in response times ought to be considered when one tracer is used as a proxy for another. Better quantification of the dependence of the patchiness parameter  $p$  on the flow parameters would enable us to exploit the  $p$ - $\tau$  relationship to estimate the response time of a tracer, or for example, the uptake time of a phytoplankton community, from the characteristics of its distribution.

[16] **Acknowledgments.** We thank T. Moore for help with the analysis of satellite data, H.A. Stone for suggesting (4), L. Seuront, L. Mémery and M. Lévy for helpful comments, W. Jenkins for helping to motivate the problem, and J. Yoder and S. Schollaert for providing the AVHRR data. The SeaWiFS and MODIS data were obtained from the NASA Goddard DAAC. This work was sponsored by ONR (N00014-00-C-0079) and NASA (NAS5-96063 and NAG5-11258).

#### References

- Abraham, E., The generation of plankton patchiness by turbulent stirring, *Nature*, 391, 577–580, 1998.
- Campbell, J., and W. Esaias, Spatial patterns in temperature and chlorophyll on Nantucket Shoals from airborne remote sensing data, May 7–9, 1981, *Journal of Marine Research*, 43, 139–161, 1985.
- Denman, K., A. Okubo, and T. Platt, The chlorophyll fluctuation spectrum in the sea, *Limnology and Oceanography*, 22, 1033–1038, 1977.
- Deschamps, P., R. Frouin, and L. Wald, Satellite determination of the mesoscale variability of the sea surface temperature, *Journal of Physical Oceanography*, 11, 864–870, 1981.
- Folt, C., and C. Burns, Biological drivers of plankton patchiness, *Trends in Ecology and Evolution*, 14, 300–305, 1999.
- Glover, D., S. Doney, A. Mariano, and R. Evans, Mesoscale variability in time-series data: Satellite based estimates of the U.S. JGOFS Bermuda Atlantic Time-series Study (BATS) site, *Journal of Geophysical Research*, (in press), 2002.
- Gower, J., K. Denman, and R. Holyer, Phytoplankton patchiness indicates the fluctuation spectrum of mesoscale oceanic structure, *Nature*, 288, 157–159, 1980.
- Lévy, M., P. Klein, and A.-M. Treguier, Impacts of sub-mesoscale physics on production and subduction of phytoplankton in an oligotrophic regime, *Journal of Marine Research*, 59, 535–565, 2001.
- Mahadevan, A., and J. Campbell, Biogeochemical variability at the sea surface: How it is linked to process response times, in *Scales in Aquatic Ecology: Measurement, Analysis and Simulation*, edited by L. Seuront and P. Strutton, CRC Press, to be published 2002.
- Mahadevan, A., and D. Archer, Modeling the impact of fronts and mesoscale circulation on the nutrient supply and biogeochemistry of the upper ocean, *Journal of Geophysical Research*, 105, 1209–1225, 2000.
- Mahadevan, A., J. Oliger, and R. Street, A non-hydrostatic mesoscale ocean model 2: Numerical implementation, *Journal of Physical Oceanography*, 26, 1181–1900, 1996.
- Platt, T., and K. Denman, Spectral analysis in ecology, *Annual Review of Ecology and Systematics*, 6, 189–210, 1975.
- Yoder, J., C. McClain, J. Blanton, and L.-Y. Oey, Spatial scales in CZCS-chlorophyll imagery of the southeastern U.S. continental shelf, *Limnology and Oceanography*, 32, 929–941, 1987.
- Yoder, J., J. Aiken, R. N. Swift, F. Hoge, and P. Stegmann, Spatial variability in the near-surface chlorophyll a fluorescence measured by the Airborne Oceanographic Lidar (AOL), *Deep Sea Research II*, 40, 37–53, 1993.
- Young, W., A. Roberts, and G. Stuhne, Reproductive pair correlations and the clustering of organisms, *Nature*, 412, 328–330, 2001.

A. Mahadevan, Ocean Process Analysis Laboratory, University of New Hampshire, and Department of Applied Mathematics and Theoretical Physics, Silver Street, Cambridge, CB3 9EW, United Kingdom. (A. Mahadevan@damtp.cam.ac.uk)

J. W. Campbell, Ocean Process Analysis Laboratory, University of New Hampshire, Durham, NH 03824, USA. (Janet.Campbell@unh.edu)